Compact, 220-ps visible laser employing single-pass, cascaded frequency conversion in monolithic periodically poled lithium niobate

A. C. Chiang, Y. C. Huang, Y. W. Fang, and Y. H. Chen

Department of Electrical Engineering, National Tsinghua University, Hsinchu 30043, Taiwan

We report the first demonstration to our knowledge of 220-ps visible laser generation from passively Q-switched-laser pumped periodically poled lithium niobate (PPLN) in a single-pass, cascaded frequency-conversion process. The monolithic PPLN consists of a 1-cm section for frequency doubling the 1064-nm Nd:YAG pump laser to a 532-nm laser and a subsequent 4-cm section for generating the visible laser in a 532-nm-pumped optical parametric generation (OPG) process. In generating the 622.3-nm OPG signal wavelength we measured a 3.0-μJ/pulse pump threshold at the 1064-nm wavelength, 16% overall efficiency, and 35% slope efficiency at two times threshold. At 10^{-6} pump duty cycle and 20-mW average power in the visible, photorefractive damage was not observed at the phase-matching temperature of 40.3 °C.   © 2001 Optical Society of America

OCIS codes: 190.2620, 190.4410, 190.4970, 140.7300, 160.4330.

Visible laser generation is important in many applications, such as spectroscopy, fluorescence excitation, and laser display. Visible gas lasers are relatively inefficient. Solid-state upconversion lasers in the visible[1-3] involve multiphoton excitation and cooperative energy transfer, which require high pumping density and offer little flexibility in wavelength tuning. We present in this Letter a novel, efficient solid-state upconversion laser at a visible wavelength.

Recent developments in passively Q-switched microchip lasers[4] have attracted wide attention for many applications. Because of its high peak power and compactness, a passively Q-switched laser (PQL) is particularly suitable for nonlinear frequency conversion. Coupled to quasi-phase-matched[5] (QPM) nonlinear optical materials, a passively Q-switched Nd:YAG laser can be an efficient pump source for producing wavelength-tunable laser radiation from optical parametric generation.[6] As a single-pass process, optical parametric generation requires only trivial laser alignment. In addition, the cost and the size of the laser are much reduced by the removal of the laser's resonator mirrors or coatings. Because optical parametric generation (OPG) is a frequency downconversion process, a Nd:YAG-laser-pumped OPG source generates laser radiation in the infrared. An attempt to generate visible OPG radiation was made by frequency doubling of a Nd:YAG PQL in a KTP crystal followed pumping of periodically poled lithium niobate (PPLN) in a subsequent stage.[7] Staging increases laser loss and difficulty of alignment. To avoid staging we employed a Nd:YAG passively Q-switched pump laser and cascaded the second harmonic generation (SHG) and the OPG in a monolithic PPLN.

We have fabricated a 0.5-mm thick, monolithic PPLN consisting of two QPM sections. The first section, responsible for frequency doubling the Nd:YAG PQL, is 1 cm long and has a 20.4-μm grating period. The 20.4-μm PPLN grating performs third-order

SHG of the 1064-nm Nd:YAG wavelength at the phase-matching temperature 40.3 °C. The second section is 4 cm long and comprises five PPLN gratings arranged parallel to the laser beam. The five gratings have periods of 11, 11.25, 11.5, 11.75, and 12 μm, each with a width of 0.9 mm, with 0.1-mm separation between adjacent gratings. To frequency double the 1064-nm Nd:YAG wavelength, the first-order QPM grating period is ~6 μm in lithium niobate. However, our electric-field poling experiment yielded repeated defects in the short-period ferroelectric domains when an ~6-μm grating region was electric-field poled, together with a long-period region in the second QPM section. We suspect that the cause of the short-period defect arises from the presence of a nonuniform poling current across the two QPM sections. Nonetheless, a PQL provides high enough peak power for performing cascaded third-order SHG and OPG, even though the efficiency of the third-order SHG is approximately one-ninth that of the first-order SHG.

Figure 1 shows the setup of the cascaded SHG–OPG experiment. The Nd:YAG passively Q-switched pump laser, made by Nanolase, generates 730-ps pulses with a peak energy of 7.5 μJ per pulse and a 3.93-kHz
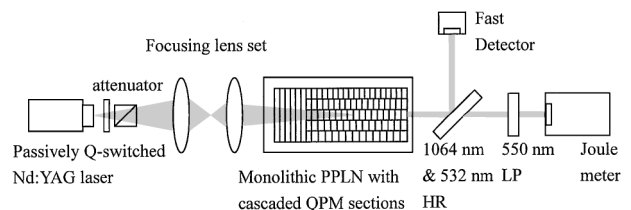

Fig. 1. Setup of the SHG–OPG cascaded QPM experiment. A passively Q-switched Nd:YAG laser pumps the first SHG PPLN section to generate a 532-nm laser, which in turn pumps the subsequent OPG section to generate visible signal lasers. The 45° high reflector (HR), made from a BK7 glass substrate, removes the 1064-nm and the infrared OPG idler energies. The long-pass filter (LP), with a cutoff wavelength at 550 nm, removes the 532-nm laser.

repetition rate. An attenuator–isolator set, consisting of a Faraday rotator following a half-wave plate, controls the pump energy and eliminates optical feedback. Two coupling lenses focus the pump laser to a 110-μm laser waist radius at the center of the OPG section. Compared with SHG, OPG requires much higher laser intensity. We therefore focused the infrared pump laser or equivalently its SHG, the 532-nm laser, onto the center of the OPG section. The oven, containing monolithic PPLN, maintains a SHG phase-matching temperature of 40.3 °C. A micrometer pushes the oven sideways to sample the QPM gratings in the OPG section and thus to tune the OPG wavelength. A 25 GHz-bandwidth InGaAs detector (New Focus, Model 1437) measures the pump laser, the pump depletion, and the generated pulse widths in a 6-GHz-bandwidth oscilloscope. In measuring the visible OPG signal, we removed the 1064-nm pump laser by using a 45° 1064-nm high reflector and the 532-nm laser by using a long-pass filter cut off at 550 nm. The infrared radiation produced from the OPG, with wavelengths of 3.7–5 μm, is absorbed by the 5-mm BK7 glass substrate of the high reflector or by the PPLN.

Figure 2(a) shows the pump pulse and the depleted pump pulse; 2(b), the 532-nm SHG pulse and the depleted 532-nm pulse; and 2(c), the visible OPG pulse at the 622.3-nm wavelength, generated from the 11-μm-period PPLN. The two end faces of the PPLN are uncoated, giving rise to 14% Fresnel reflection from each end face. All the vertical axes are scaled to the internal laser powers in the PPLN, where the internal pump energy at the 1064-nm wavelength is fixed at 6.54 μJ/pulse. As can be seen from Fig. 2(a), approximately 75% of the 1064-nm pump laser is converted into the 532-nm SHG laser in the first QPM section. The FWHM pulse width of the infrared pump is ~730 ps. For the SHG process in the first QPM section, the effective nonlinear coefficient measured in the experiment is ~80% of its theoretical value. Figure 2(b) shows the 532-nm SHG pulse and the corresponding OPG depleted pulse. The 532-nm laser pulse width, ~535 ps, is ~1.35 times reduced from the 730-ps infrared pump pulse width. Because of the OPG exponential gain, the peak depletion at the center of the 532-nm laser pulse is more than 60%. Figure 2(c) shows the corresponding 622.3-nm OPG pulse with a FWHM pulse width of 220 ps, or 3 cm inside lithium niobate (extraordinary refractive index for lithium niobate, 2.16). The OPG pulse width is greatly reduced from the 532-nm pump pulse width owing to the OPG exponential gain expression in the high-gain regime. As the 532-nm pump pulse length is only 7 cm inside the 5-cm PPLN and the second QPM section starts 1 cm from the infrared pump edge, parametric amplification from Fresnel reflections at the two PPLN end faces is negligible. Indeed, we observed a comparable OPG power when we tilted the PPLN with a small angle in the horizontal plane, although we had to change the oven temperature slightly to restore the phase-matching condition.

Figure 3 shows the short OPG wavelength versus the grating period in the second QPM region. Be-

fore taking data, we calibrated a CVI DK480 0.5-m monochromator against the 632.8-nm He–Ne and 532-nm laser wavelengths. The experimental data, designated by the open circles in Fig. 3, are compared with the published Sellmeier equation[8] designated by a solid curve in the same figure. The plot shows ~1-nm discrepancy in wavelength. To resolve the discrepancy, we investigated the wavelength sensitivity against temperature and grating period. We found that it takes a temperature reduction of 30 °C
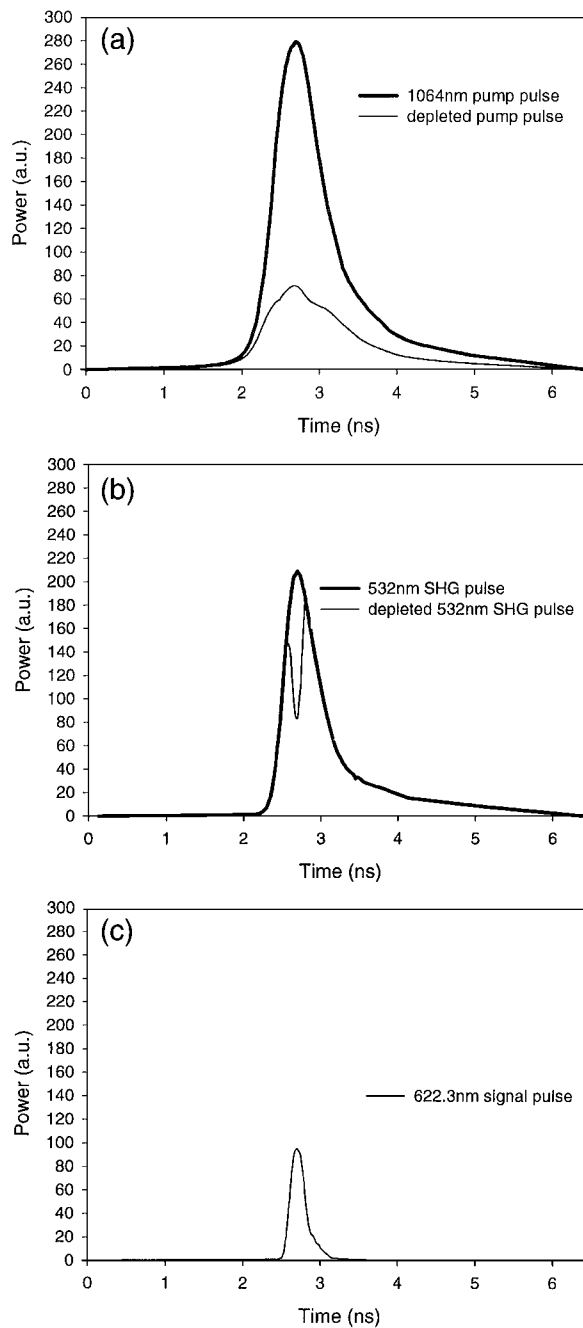

Fig. 2. (a) 1064-nm pump pulse (FWHM, ~730 ps) and the depleted 1064-nm pump pulse, (b) 532-nm SHG pulse (FWHM, ~510 ps) and the depleted 532-nm pulse, (c) 622.3-nm visible OPG signal pulse (FWHM, ~220 ps). The vertical axes are scaled to the internal laser powers in the PPLN, where a 6.54-μJ/pulse internal pump energy at the 1064-nm wavelength is fixed for all plots.
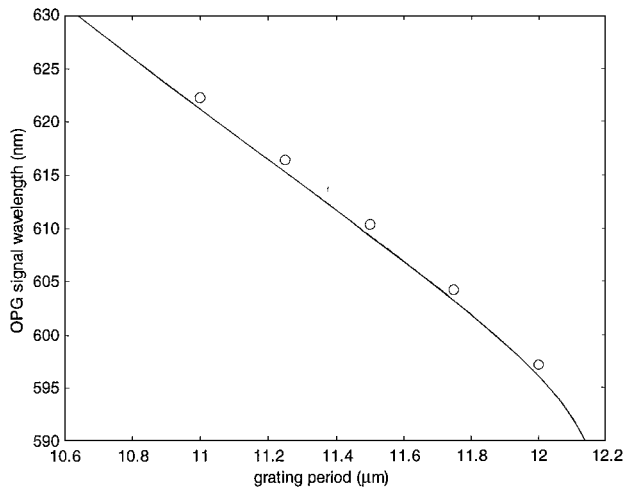
Fig. 3. Calculated (solid curve) and measured (open circles) OPG visible wavelengths. The ~1-nm wavelength discrepancy in the vertical axis is likely attributable to 0.04-μm uncertainty in the PPLN grating period.
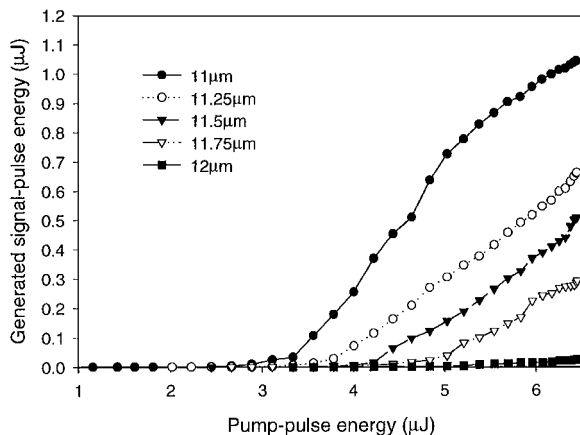

Fig. 4. Measured OPG signal energy versus 1064-nm pump energy for the five OPG grating periods. As the grating period becomes increasingly longer, the OPG idler wavelength moves into the absorption region of the PPLN, and the OPG signal energy is reduced. For the 11-μm grating period, the 1064- to 622.3-nm laser conversion efficiency is 16.5%, and its slope efficiency is 35%.

or a grating-period reduction of 0.04 μm to match the experimental data with the published Sellmeier equation. Therefore the discrepancy is most probably attributable to the precision of the grating periods in our lithographic mask.

Figure 4 shows the pulse energy of the visible OPG versus the infrared pulse energy at the 1064-nm wavelength. All the values in the figure have been converted to the internal energies in the PPLN. For pumping by the 532-nm laser at 40.3 °C, the multiple PPLN gratings generate the signal and idler wavelength pairs [622.3, 3666 nm], [616.4, 3885 nm], [610.4, 4160 nm], [604.2, 4452 nm], [597.1, 4879 nm] that correspond to the grating periods 11, 11.25, 11.5, 11.75, and 12 μm. As congruent lithium niobate absorbs laser energies with their wavelengths

longer than 4 μm, the pump threshold is increasingly higher when the mid-infrared idler wavelength becomes longer. At the PQL's internal pump energy of 6.45 μJ/pulse, the overall conversion efficiency from the infrared to 622.3 nm is 16.5%, resulting from 75% SHG conversion efficiency in the first QPM section and 22% OPG signal efficiency in the second QPM section. When both the signal and the idler laser energies are included, the total OPG efficiency is 26%. The parametric gain exceeds 10^{12}. The maximum slope efficiency, which also occurs at the 622.3-nm output, is ~35%. The effective nonlinear coefficient in the OPG section is estimated by a plane-wave approximation[9] to be 15.5 pm/V. The experimental nonlinear coefficient in the second QPM section is ~91% of the theoretical value.

In conclusion, we have demonstrated the generation of a short-pulse visible laser by using a SHG and OPG cascaded process in monolithic PPLN. The laser is pumped by a 730-ps passively Q-switched Nd:YAG laser at a 1064-nm wavelength. The cascaded nonlinear process generates 220-ps visible laser radiation from 597 to 622 nm at a 3.93-kHz repetition rate. The monolithic PPLN consists of a 1-cm, third-order QPM SHG section and a 4-cm OPG section. To achieve maximum parametric gain while having enough SHG power at the 532-nm wavelength, we focused the infrared pump laser waist to the center of the OPG section. At the 622.3-nm visible OPG wavelength, the SHG conversion efficiency is ~75% and the OPG efficiency is ~26% with 6.45-μJ/pulse internal pump energy at the 1064 nm wavelength.

References

1. R. J. Trash and L. F. Johnson, in *Compact Blue/Green Lasers*, Vol. 6 of 1992 OSA Technical Digest Series (Optical Society of America, Washington, D.C., 1992), paper ThB3.
2. T. J. Whitley, C. A. Millar, R. Wyatt, M. C. Brierley, and D. Szebesta, Electron. Lett. **27,** 1785 (1991).
3. H. Scheife, T. Sandrock, E. Heumann, T. Danger, and G. Huber, in *Advanced Solid-State Lasers*, C. R. Pollock and W. R. Bosenberg, eds., Vol. 10 of OSA Trends in Optics and Photonics Series (Optical Society of America, Washington, D.C., 1997), pp. 79–82.
4. J. J. Zayhowski, in *Miniature Coherent Light Sources in Dielectric Media*, D. C. Hanna and B. Jacqier, eds. (Elsevier, Amsterdam, 1997), pp. 255–267.
5. M. M. Fejer, G. A. Magel, D. H. Jundt, and R. L. Byer, IEEE J. Quantum Electron. **28,** 2631 (1992).
6. J. J. Zayhowski, Opt. Lett. **22,** 169 (1997).
7. U. Bader, J.-P. Meyn, J. Bartschke, T. Weber, A. Borsutzky, R. Wallenstein, R. G. Batchko, M. M. Fejer, and R. L. Byer, Opt. Lett. **24,** 1608 (1999).
8. D. J. Jundt, Opt. Lett. **22,** 1553 (1999).
9. B. E. A. Saleh and M. C. Teich, *Fundamental of Photonics* (Wiley, New York, 1991), pp. 771–773.